Biointerface Research in Applied Chemistry
Platinum Open Access Journal (ISSN: 2069-5837)

Article
Volume 11, Issue 4, 2021, 11256 - 11271
https://doi.org/10.33263/BRIAC114.1125611271

Effects of Humic Acid and Natural Sunlight Irradiation on the Behaviour of Zinc Oxide Nanoparticles in the Aqueous Environment

Valach Andrian Velintine [1], Boon Siong Wee [1,*], Eric Kwabena Droepenu [1], Suk Fun Chin [1], Kuan Ying Kok [2]

[1] Chemistry Programme, Faculty of Resource Science and Technology, Universiti Malaysia Sarawak, Kota Samarahan, 94300, Sarawak, MALAYSIA; veevelintine@gmail.com (V.A.V.); swboon@unimas.my (B.S.W.); kobladodzie01@yahoo.com (E.K.D.); sfchin@unimas.my (S.F.C.);
[2] Malaysian Nuclear Agency, Bangi, Kajang, 43000 Selangor, MALAYSIA; kyk1000@nuclearmalaysia.gov.my (K.Y.K.);
* Correspondence: swboon@unimas.my;

Scopus Author ID 57194506096
Received: 12.11.2020; Revised: 6.12.2020; Accepted: 8.12.2020; Published: 10.12.2020

Abstract: The unique properties of ZnO nanoparticles have attracted scientists' interest to produce on a large-scale. Household items, cosmetics, consumer products, and electric sensors are some products that utilize these ZnO nanomaterials. Eventually, ZnO nanoparticles will be released into the environment in various ways. Once released, ZnO nanoparticles would dissociate into Zn^{2+} ions, which are toxic to aquatic organisms. The presence of humic acid and exposure to sunlight could affect the dissolution of ZnO nanoparticles. Two sizes of commercial ZnO nanoparticles (< 50 nm and < 100 nm) were chosen to study the influence of humic acid and sunlight on the dissolution. In the presence of humic acid, the dissolution of both sizes is higher, with 67 % and 39 % Zn^{2+} dissolved for < 50 nm and < 100 nm, respectively. The concentration of Zn^{2+} ions seems to be consistent or stable when exposed to sunlight. However, the humic acid enhanced the release of Zn^{2+} ions. Langmuir isotherm model best fitted for the humic acid's sorption onto the ZnO nanoparticles with the process been favorable.

Keywords: ZnO nanoparticles; humic acid; sunlight; dissolution; aggregation.

© 2020 by the authors. This article is an open-access article distributed under the terms and conditions of the Creative Commons Attribution (CC BY) license (https://creativecommons.org/licenses/by/4.0/).

1. Introduction

Applications of nanotechnology in daily usage are already well known [1-6]. To date, nanomaterials' production has become more rapid and on a large scale by years, which consequently increased the amount released to the environment [7-10]. For instance, nanoscale materials' production is expected to exceed $125 billion by 2024 [11]. These nanoscale metal oxides exhibit unique physical and chemical properties essential for their applications [12-14]. For example, zinc oxide and titanium dioxide were used in cosmetic and sunscreen products due to their ability to absorb UV light [15-16] and antibacterial activity [17-19]. ZnO and TiO_2 nanoparticles were also widely used as catalysts in water treatment [20], removing pollutants such as dye and humic acid [21-22].

Climate change and hydrological processes could affect the biodegradable activity of dead plants, determining the concentration of organic matter released into the aquatic ecosystem. According to [23], natural organic matters are present in almost all aquatics ecosystems. The concentration is ranging from 0.1 – 10.0 ppm depending on biogeochemical conditions and climate. Natural organic matter consists of fractions of humic substances such

as high molecular weight organic molecules (humic acid), soluble in water at pH >2; humin, insoluble in all pH, and fulvic acid, soluble in all pH [24-25]. However, these organic molecules contain a high abundance of functional groups such as phenolic, carboxylic, hydroxyl, amine, and quinine groups [26], which bind to metal oxide surfaces in water to enhance their mobility. Similarly, the presence of humic acid (HA) can react with chlorine in the water to produce by-products such as trihalomethane, a carcinogenic substance [27]. In aqueous suspension, any metal oxide nanoparticles have surface sites that are protonated or deprotonated, depending on the pH value. According to [7,28-29], the adsorption of natural organic matter affecting the surface speciation and net charge of the particles influences their stability, determining their fate, transport, behavior, and bioavailability. Functional groups' presence in the HA structure gave a strong affinity for metal cations, leading to complexation with metal cations [26].

ZnO nanoparticles are preferred to TiO_2 because both have similar catalytic properties of a semiconductor. However, ZnO exhibits higher electron mobility and a longer photo-generated electron lifetime than TiO_2 in the degradation of dyes [30]. ZnO nanoparticles can also undergo excitation at room temperature under low excitation energy and absorb a larger fraction of the solar spectrum than TiO_2 [31]. Also, in large scale operations, ZnO nanoparticles are low cost, non-toxic, and biocompatible [32]. According to [33], most semiconductors release metal ions during photocatalysis, which poses secondary pollution as well as their interaction with other pollutants. Even though sunlight enhances the photocatalytic properties, it is a concern whether ZnO's properties in the presence of sunlight might enhance the ecological toxicity by releasing more zinc ions under natural environmental conditions [34]. There are fewer reports on the effects of natural sunlight and HA on ZnO nanoparticles' behavior in an aqueous environment [35-39]. Therefore, this study aimed to investigate the influence of HA and natural sunlight on ZnO nanoparticles' behavior in the aquatic environment.

2. Materials and Methods

2.1. Chemicals.

In this study, zinc oxide (ZnO) nanoparticles of different sizes (< 50 nm and < 100 nm) were obtained from Sigma-Aldrich. On the other hand, HA used in this experiment was purchased from Sigma-Aldrich, Switzerland. Sodium hydroxide (NaOH; Amresco, Ohio) and nitric acid (HNO_3; Fisher Chemicals) of concentration 1.0 M were used to adjust sample solutions' pH. Changes in pH were measured using Martini Instruments (Model Mi 150) pH meter. Deionized water was used to prepare solutions, and analytical reagent grade chemicals are used without purification.

2.2. ZnO nanoparticles size distribution.

The particle size distribution of ZnO nanoparticle samples was analyzed using Transmission Electron Microscopy (TEM) (JEOL model JEM – 1230) using the modified preparation procedure based on previous studies [40]. Briefly, the ZnO nanoparticles stock solution was sonicated for 30 minutes to ensure better dispersion among aggregated particles. About 15 µL sample solutions were dropped onto coated copper grids and left to dry overnight before viewed under TEM.

2.3. Humic acid (HA) preparation.

Preparation of HA adopted the method reported by [41], with some modifications. A stock solution of humic acid (100 mg/L) was prepared by dissolving a calculated amount in an alkaline solution (pH 9) to enable efficient dissolution [42]. From the stock, 10 mg/L solutions were prepared, and the pH was adjusted using HCl and NaOH solutions. The content was stirred on an electric hotplate magnetic stirrer (Fisherbrand) for 24 hours. Diluted solutions of the HA of different concentrations were prepared and analyzed using UV/ Visible spectrophotometer (UV-1800 SHIMADZU) at a wavelength of 254 nm [43]. A calibration curve was determined using standardized HA solutions as reported by [44] with a slight modification in the procedure. All stock solution was kept in the fridge and out of light source when not in use.

2.4. Adsorption study.

To understand HA's adsorption behaviors on the surface of ZnO nanoparticles, < 100 nm ZnO was chosen instead of the < 50 nm ZnO samples to avoid total dissolution at lower pH. 5 mg of ZnO powder was added to 5 mg/L of HA solution of different pH (1, 3, 5, 7, 9, 11) and stirred at 150 rpm for 24 hours. After the 24-hour equilibrium, each suspension was filtered using 0.45 µm filter paper to remove bigger particulates. The filtrates were analyzed using UV/ Visible spectrophotometer and Atomic Absorption Spectrometer (AAS) for residual concentrations. The amount adsorbed, Q (mg/kg), was calculated using the formula reported by [45]:

$$Q = \frac{(C_0 - C_t)V}{w} \quad (1)$$

where;

C_0 and C_t (mg/L) is the liquid-phase concentrations of HA at initial and at any given time, respectively. V (L) is the solution's volume, and w (kg) is the mass of ZnO nanoparticles. The adsorption equilibrium data obtained from the study were analyzed using Langmuir and Freundlich's isotherm models reported by [46] in equations 2 and 4.

$$\frac{C_e}{q_e} = \left[\frac{1}{Q_o K}\right] + \frac{C_e}{Q_o} \quad (2)$$

where,

C_e – equilibrium concentration, mg/g, q_e – amount absorbed at equilibrium, mg/g, Q_o, and K – Langmuir constants relating to adsorption capacity and energy of adsorption, which was determined from the slope and intercept of the linear plot of C_e/q_e Vs. C_e.

The essential features of a Langmuir isotherm can be expressed in terms of a dimensionless constant separation factor or equilibrium parameter, R_L, that is used to predict if an adsorption system is “favorable” or “unfavorable”. The separation factor, R_L is defined by [47] and represented with the Equation:

$$R_L = \frac{1}{1+KC_o} \quad (3)$$

where,

C_o – sorbate concentration, mg/l, K – Langmuir adsorption equilibrium constant, L/g. The isotherm is unfavorable when $R_L>1$, the isotherm is linear when $R_L=1$, the isotherm is favorable when $0<R_L<1$, and the isotherm is irreversible when $R_L=0$ [48].

$$\log q_e = \log K_f + \frac{1}{n}\log C_e \quad (4)$$

where,

q_e – amount adsorbed at equilibrium, mg/g, C_e – equilibrium concentration, mg/l, K_f, and n – Freundlich model constants. These constants can be obtained from the slope and intercept of the plot of log q_e against log C_e.

2.5. Sunlight irradiation experiments.

The 0.2 g/l ZnO nanoparticles stock solution was prepared by dissolving ZnO nanoparticles powder in deionized water. The solution was sonicated for 30 minutes to get a better dispersion of particles.

To study the dissolution of ZnO nanoparticles influenced by sunlight in the presence and absence of humic acid, 0.2 g/L stock solution of ZnO was prepared according to the method reported by [35,49]. A 50 ml volume of each of the ZnO stock solution and 50 ml of 100 mg/L HA solutions were sonicated for 10 minutes using Ney ULTRAsonik (20 KHz; 200 W/L) before adjusting the solution pH to the desired value. Samples were prepared by using a range of solution conditions: pH 1 – 9; ionic strength (I) 0 – 5 mM. A concentration of 1.0 M NaCl was used to adjust the ionic strength of the solutions. The pH value was measured using Martini Instruments (Model Mi 150) pH meter. Sunlight irradiation experiment was done from 9 am to 5 pm for two consecutive days. The ambient temperature was 28°C ± 3°C during the experiment. Sunlight intensity was measured using Easy View 30 light Meter (in Lux unit). Dissolution measurement was obtained for every two-hour intervals during two days of exposure. Sunlight intensity was measured every hour of exposure with an average of 0.012 Watt cm^{-2} after conversion from Lux unit to Watt cm^{-2} (at 555 nm). Total dissolved Zn^{2+} ion in samples was analyzed using Perkin Elmer Optima 8000 inductively coupled plasma optical emission spectrometer (ICP – OES). At night, the exposed samples were kept in the dark cabinet away from light to prevent degradation. Control experiments were also prepared with the same methods as described above. Instead of exposure to light, the samples were stored in a dark cabinet.

3. Results and Discussion

3.1. Particle size distribution.

The average diameter determined for the two ZnO nanoparticles samples (< 50 nm and < 100 nm) from the TEM analysis were 45 ± 24 nm and 85 ± 36 nm respectively. The particle size distribution is illustrated in Figure 1. The results confirmed that the < 100 nm ZnO nanoparticles were more dispersed compared to the < 50 nm ZnO nanoparticles. Inlet Figures show the TEM images that were used to calculate the particle size distribution.

On the other hand, the interaction of the ZnO nanoparticles to HA showed the HA's complexation ability as this was analyzed using TEM shown in Figure 2. According to [26], the presence of functional groups such as carboxyl, hydroxyl, and phenol enables HA to form strong complexations with heavy metal ions in aqueous solutions. The figures also reveal that HA caused the smaller sized ZnO nanoparticles (< 50 nm) to aggregate more to form bigger clusters [50]. In contrast, the larger sized ZnO nanoparticles (< 100 nm) did not show greater cluster but rather showed less clustered aggregates in the presence of HA.

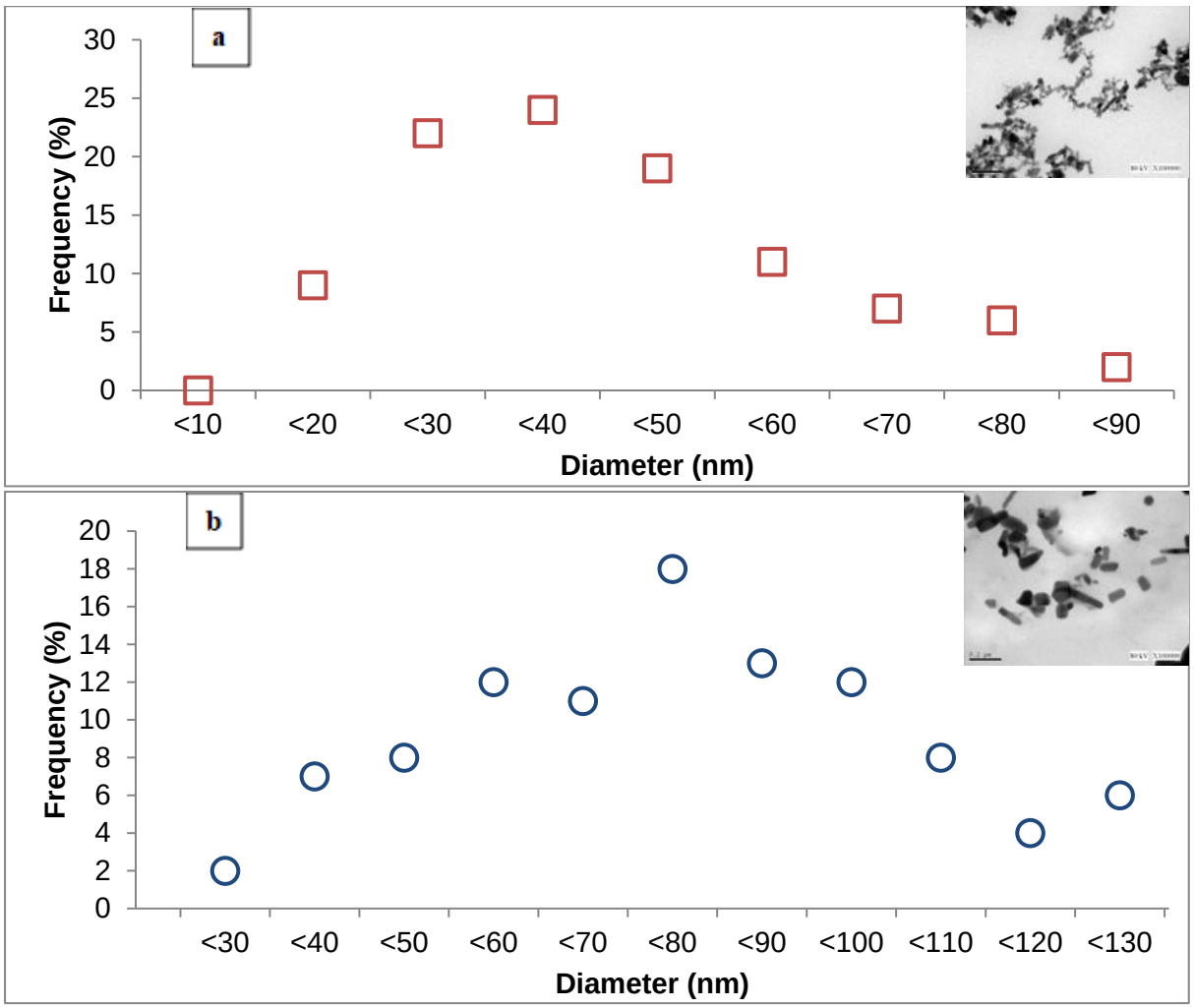

Figure 1. Particle size distribution (TEM) for (**a**) < 50 nm ZnO (mean 45 ± 24 nm, n = 247); (**b**) < 100 nm ZnO (mean 85 ± 36 nm, n = 190) displayed as percentage of total count. Inlet is the TEM images of pre-sonicated ZnO nanoparticles.

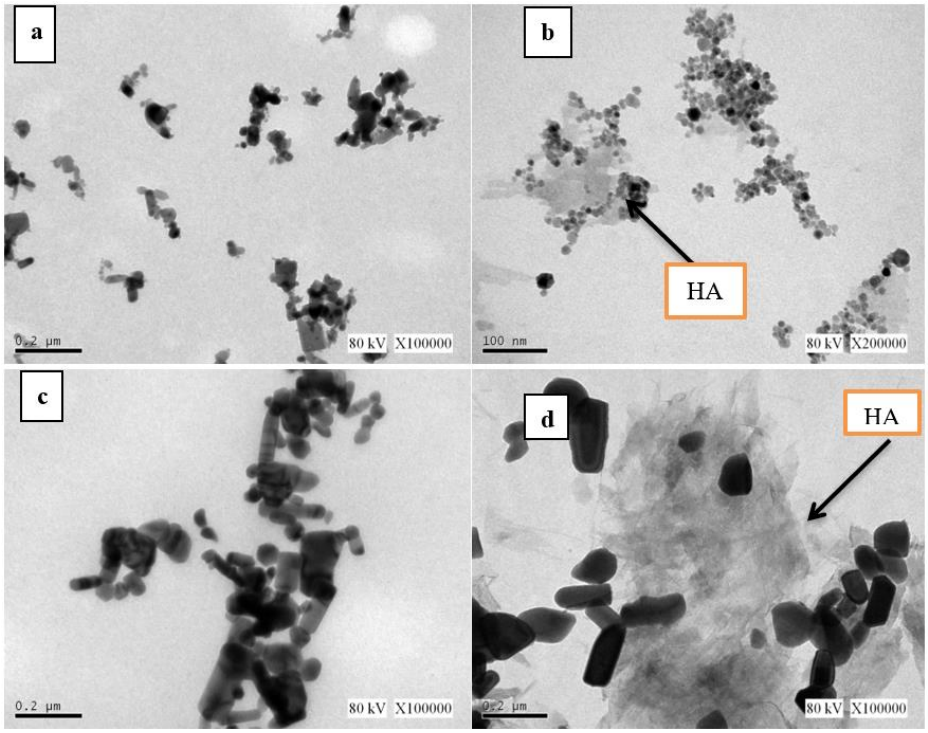

Figure 2. Complexation of ZnO nanoparticles when < 50 nm sample in the (**a**) absence of HA; (**b**) presence of HA; < 100 nm sample in the (**c**) absence of HA; (**d**) presence of HA [Ionic strength = 3 mM at 0 h].

3.2. Adsorption of humic acid on ZnO nanoparticles surface.

Studies were carried out to determine the adsorption effect between ZnO nanoparticles and HA at different pH (pH 1, 3, 5, 7, 9). The initial concentration of 5 mg/L of HA was chosen based on the total dissolved solids (HA) concentration of Paka river Terengganu, Malaysia, between 0.02 and 4.17 mg/L [24,51]. Figure 3 illustrates the amount of HA adsorbed onto the ZnO nanoparticles and the concentration of Zn^{2+} ions released during the adsorption experiment.

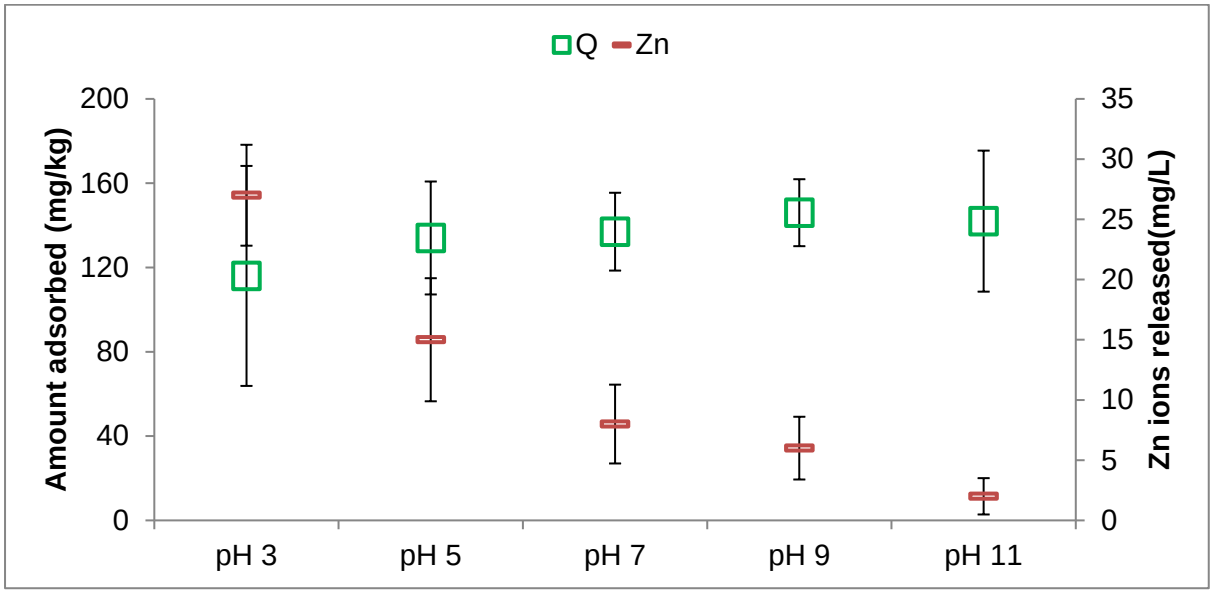

Figure 3. Amount of HA adsorbed onto ZnO nanoparticles (Q) and concentration of Zn^{2+} ions released during the adsorption experiment.

From the result, increasing pH results in a decrease in Zn^{2+} ions production in the solution medium. The highest Zn^{2+} ion produced occurred at a pH of 3 with a concentration of 27 mg/L, whereas, at a pH of 11, only about 2 mg/L Zn^{2+} ions were generated. This implies that, at higher pH, more ZnO nanoparticles are present in the solution medium than their dissolved ions. A direct response exists between ZnO surfaces and protons in acidic conditions, causing the ZnO nanoparticles to dissolve more [52-54]. In a study by [55], ZnO thin films' dissolution behavior was investigated under different pH. From their findings, the dissolution rate of the magnetron-sputtered ZnO thin films was moderate at pH 6 and decreased markedly at pH 7 increased. The trend continued to decrease to pH 10 and finally increased with further increase in the pH. Their result was similar to the trends observed in the ZnO nanoparticles used in this study. The dissociations of ZnO can be expressed by the following reactions suggested by [35,52,55];

$$ZnO(s) + 2H^+ \leftrightarrow Zn^{2+} + H_2O_{(l)} \quad (1)$$

$$ZnO(s) + H^+ \leftrightarrow ZnOH^+ \quad (2)$$

As pH approaches neutrality (7), the H^+ ions decrease, thereby reducing the frequency of proton attacks. The solubility of ZnO nanoparticles eventually decreases as pH increases between 7 – 9 as hydroxide groups are produced in the solution medium according to [56] with the reaction:

$$ZnO(s) + OH^- + H_2O_{(l)} \leftrightarrow Zn(OH)_3^- \quad (3)$$

$$ZnO(s) + 2OH^- + H_2O_{(l)} \leftrightarrow Zn(OH)_4^- \quad (4)$$

Further dissolution was inhibited by the hydroxide layer formed on the ZnO surface under alkaline conditions. According to [55], reaction equations (3) and (4) suggest that ZnO formed hydroxo complexes with OH^- in alkaline conditions.

On the contrary, the solubility of HA increases with increasing pH [42]. In this instance, more dissolved HA forms complexes on the surface of the ZnO nanoparticles, thereby, increasing its sorption capacity. This was depicted by the plot in Figure 3 where at a pH of 11, the maximum amount of HA adsorbed was recorded (146 mg/g). However, since less HA was dissolved at lower pH, only a few amounts of the bulky HA (116 mg/g) could be adsorbed on the surfaces of the adsorbent. This result contradicts the study by [57]. In their study, they concluded that an increase in HA concentration and pH decreased the removal efficiency of ZnO nanoparticles in water. This resulted from the increased generation of hydrogen radicles at lower pH, which attacked the aromatic rings of the HA to break the carbon-hydrogen bonds by the UV light, which provided the energy for this mechanism.

The adsorption isotherm of HA onto ZnO nanoparticles was also studied using Langmuir and Freundlich isotherms. The plots are illustrated in Figure 4.

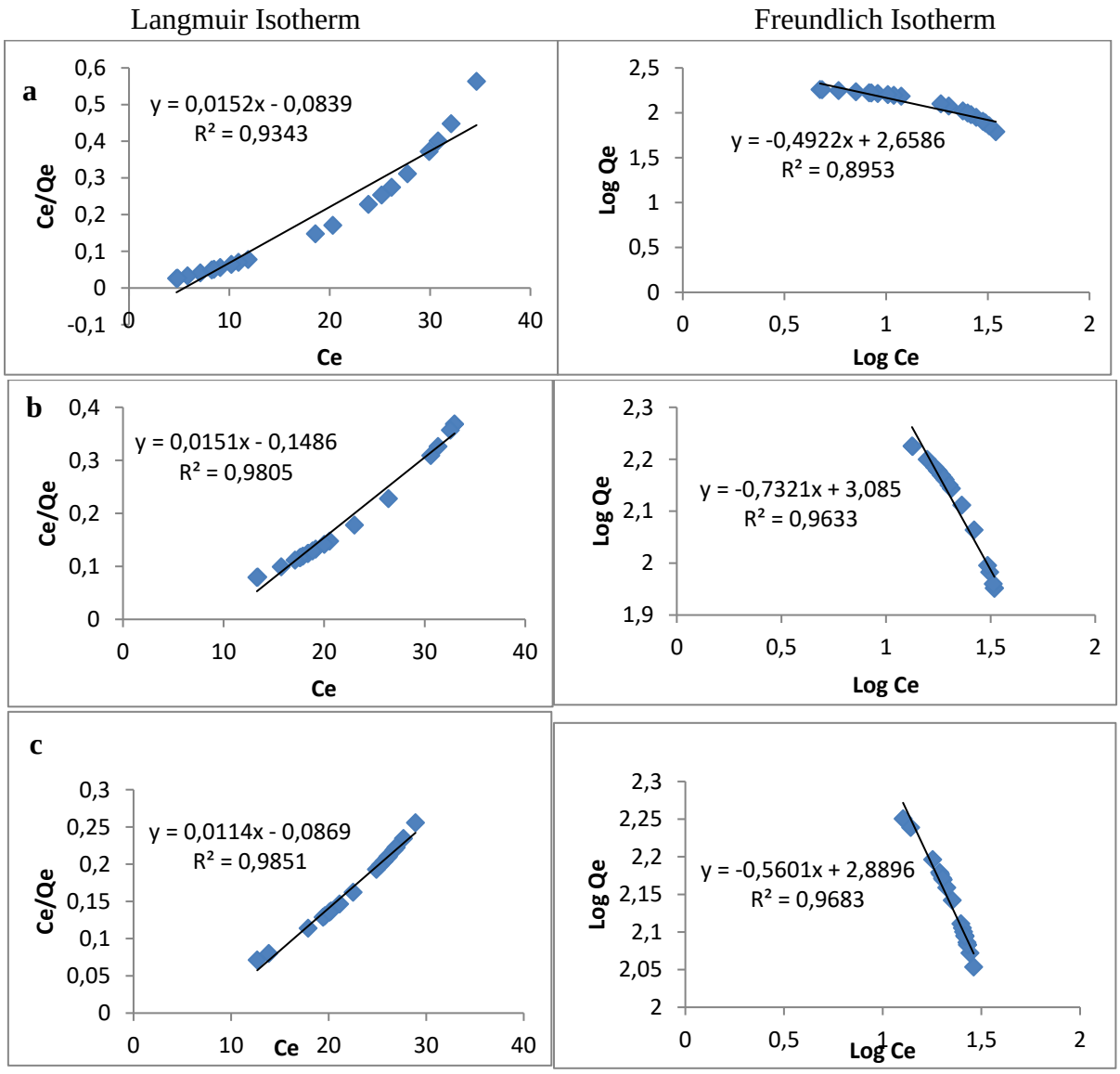

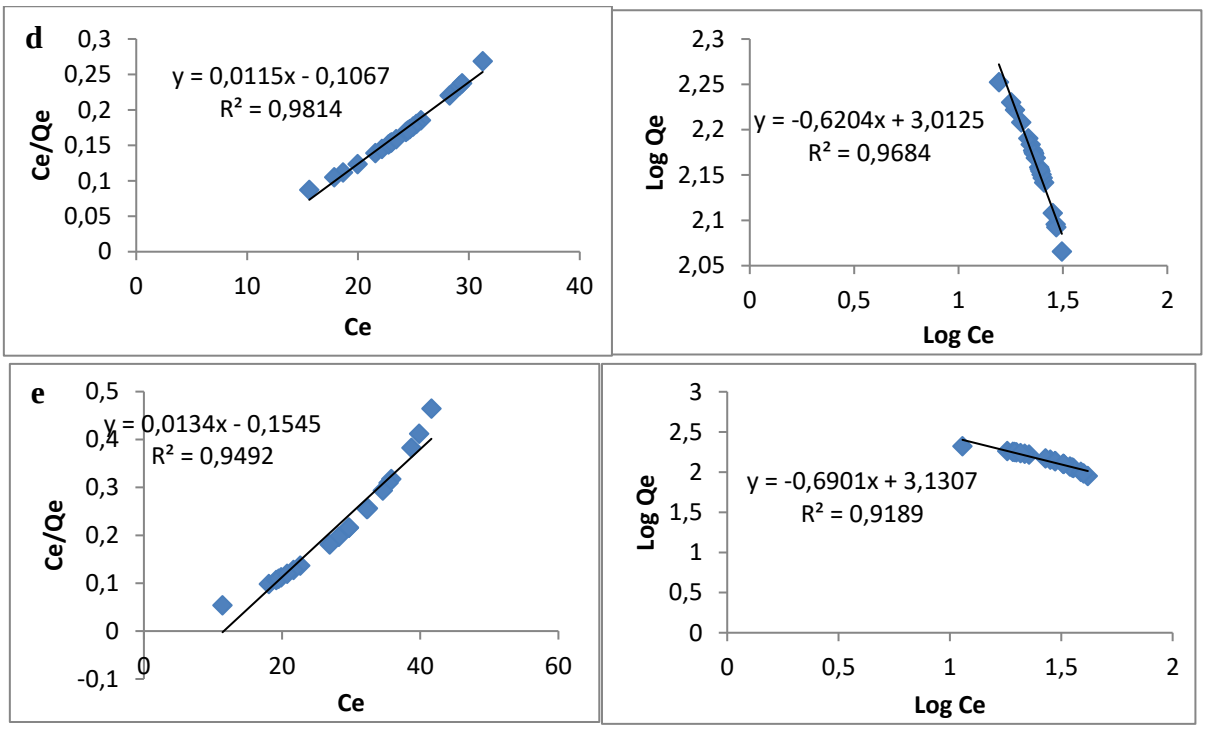

Figure 4. Graph of Langmuir and Freundlich adsorption isotherms of humic acid onto ZnO nanoparticles at (**a**) pH 3, (**b**) pH 5, (**c**) pH 7, (**d**) pH 9; (e) pH 11.

The constant parameters, regression correlation coefficient (R^2), and separation factors calculated for the two isotherm models are tabulated in Table 1.

Table 1. Langmuir and Freundlich isotherms fitting parameters

Solution pH	Langmuir Isotherms constants			Freundlich isotherms constants			
	R^2	K_L	R_L	R^2	K_f	1/ n	n
3	0.9343	65.7890	0.0003	0.8953	455.6170	-2.0317	-2.0317
5	0.9805	66.2250	0.0002	0.9633	1216.1860	-1.3659	-1.3659
7	0.9851	59.5200	0.0003	0.9683	775.5000	-1.7853	-1.7853
9	0.9814	86.9560	0.0002	0.9684	1029.2000	-1.6112	-1.6119
11	0.9492	74.626	0.0002	0.9189	1351.13	1.4490	1.4490

The correlation coefficient (R^2) obtained from Langmuir isotherm at all pH is between 0.9343 to 0.9851 compared to 0.8953 to 0.9684 recorded for Freundlich isotherm. This presupposes that the Langmuir isotherm model fits well for the adsorption process, which aligned with the study by [58]. Again, the sorption process was favorable due to the separation factor (R_L), which fell between 0 and 1. On the other hand, according to Freundlich's model, the process was unfavorable except for the dataset for pH 11, which had its constant "n" above 1. This is because, if $n < 1$, it suggests that the sorption process is unfavorable, and if $n > 1$, the process is considered to be favorable [48,59].

3.3. Effect of HA on the dissolution of ZnO nanoparticles.

Figure 5 shows dissolved Zn^{2+} ions released from two different sizes of ZnO nanoparticles in the presence and absence of HA at different pH for two days. Results show that the concentration of Zn^{2+} ion released from smaller sized ZnO nanoparticle (< 50 nm) were higher (67 mg/L) than ions released from larger sized ZnO nanoparticles (< 100 nm) of 13 mg/L at pH 1 for both samples. In the presence and absence of HA for the smaller ZnO nanoparticles (< 50 nm), dissolution decreases with increasing pH for days 1 and 2. In the case of the larger particle size (< 100 nm), dissolution decreased from pH 1 to pH 7. Eventually, it

increased to about 28 mg/L for days 1 and 2 in the presence of HA. However, in the absence of HA, the decreased dissolution began from pH 1 to pH 6, peaked at pH 7, and finally decreased in pH 9. This result is in line with a study by [60], which attributed the higher dissolution to agglomeration and sedimentation.

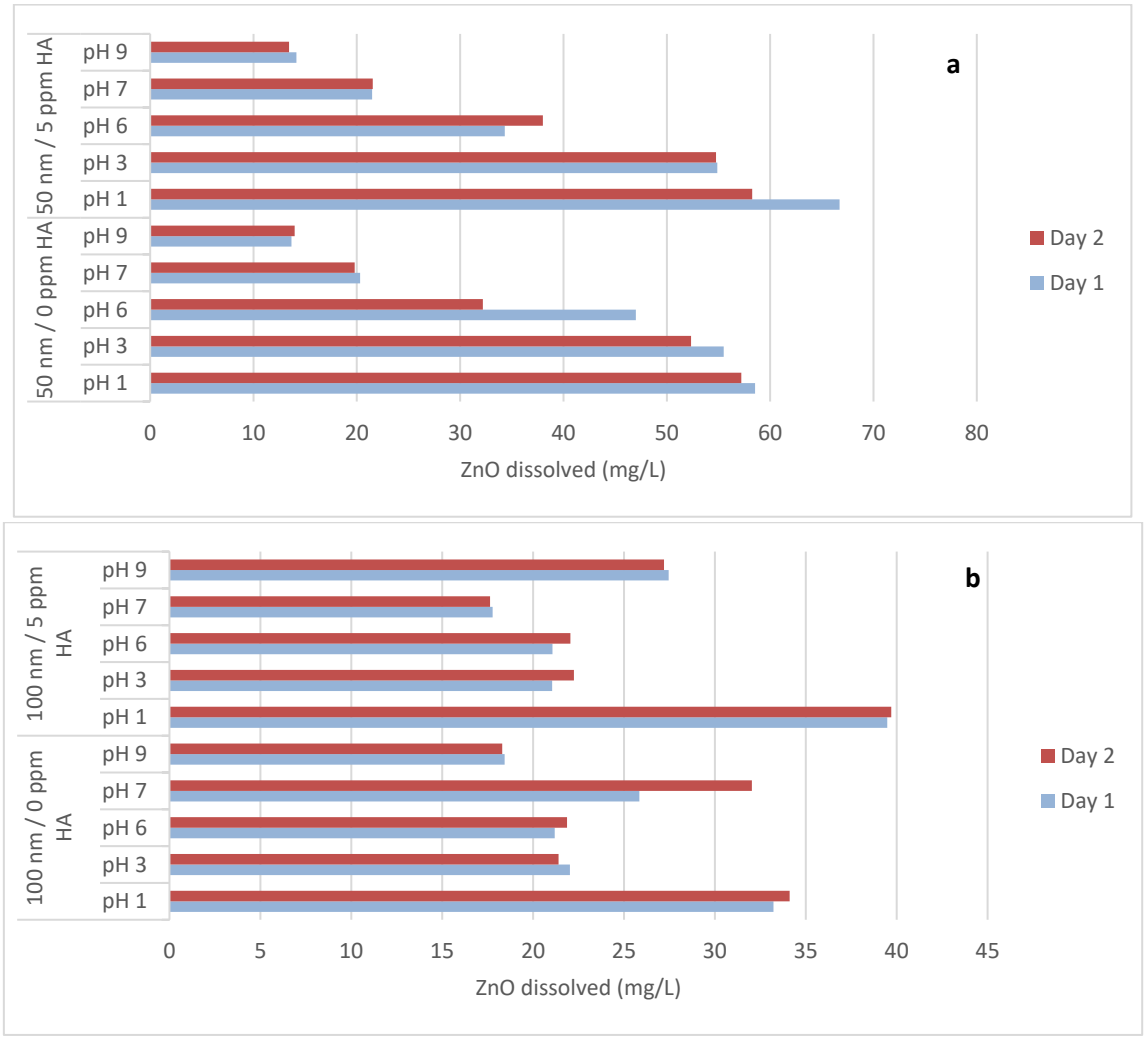

Figure 5. Dissolution of ZnO nanoparticles; (**a**) < 50 nm; (**b**) < 100 nm in the presence and absence of HA at different pH conditions for two days; ionic strength = 3 mM NaCl.

This finding was also in agreement with previous studies by [54]. More than 53% of ZnO nanoparticles were dissolved as Zn^{2+} ions at pH 3-6. However, at pH 8-11, the ZnO nanoparticles' solubility was reduced to less than 5%. According to [54], adsorption of HA on ZnO nanoparticle surfaces reduces the particles' surface potential due to negatively charged HA. Meanwhile, it was reported that HA increased the dissolution of ZnO at high pH (9 and 11) as bonding between the HA and the sorbate ions lose their polarity [61]. Previous studies regarding the effect of size and dissolution have been carried out. However, there is less study that involves different pH when HA present. TEM images in Figure 3a and 3c shows how this size-factor related to the solubility of particles. Larger sized particles (< 100 nm) are less soluble than smaller sized particles (< 50 nm), and this is shown when they tend to aggregate with themselves.

3.4. Effect of sunlight on the dissolution of ZnO nanoparticles.

Figure 6 shows the effect of sunlight in the dissolution of ZnO nanoparticles (< 50 nm and < 100 nm) in the (a) presence and (b) absence of HA at a specific pH of 7 and ionic strength

(I) of 3 mM NaCl. The < 50 nm and < 100 nm ZnO nanoparticles were more stable in the presence of sunlight and HA than in the absence of sunlight and HA. The dissolution of the two ZnO samples (< 50 nm and < 100 nm) in the presence of HA and sunlight remains constant in the range of 21.41-21.83 mg/L and 17.53-17.77 mg/L, respectively. However, the smaller particles (< 50 nm) in the presence of HA with no sunlight saw an increase in Zn^{2+} ion release within the first 4 hours of irradiation with a maximum yield of 28.07 mg/L. This then decreased gradually to 9.37 mg/L at the 32nd hour of irradiation.

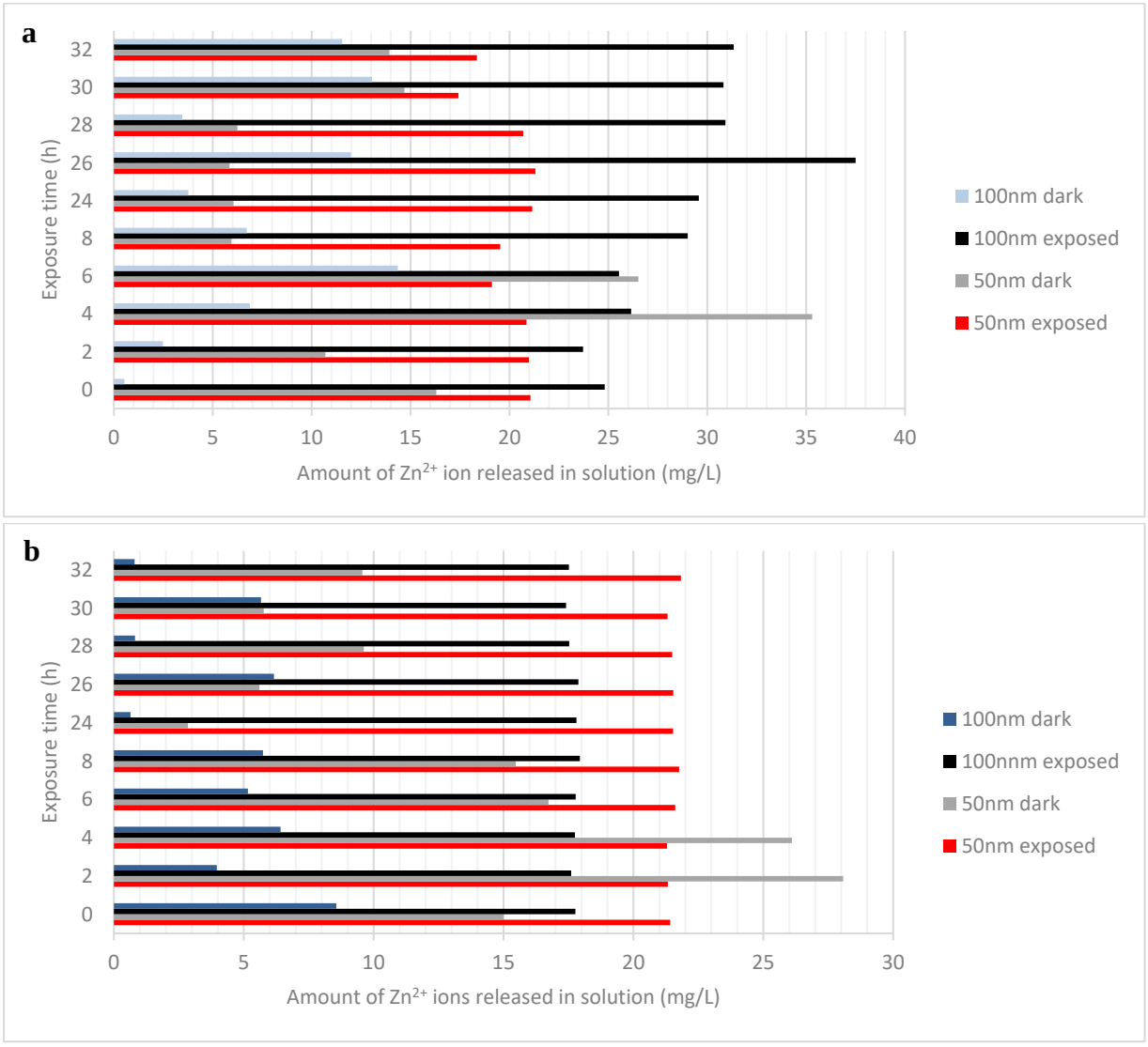

Figure 6. Effect of sunlight in the dissolution of ZnO nanoparticles at pH 7 in (**a**) HA = 0 mg/L; (**b**) HA = 5 mg/L, I = 3 mM NaCl.

In the absence of sunlight, the smaller ZnO nanoparticles (< 50 nm) increased in their dissolutions in the presence and absence of HA for the first 4 hours of irradiation and gradually decreased. The maximum concentrations of Zn^{2+} generated in solution in the absence and presence of HA were 35.31 mg/L and 28.07 mg/L, respectively. However, in the absence of sunlight, dissolution of < 100 nm ZnO sample to produce Zn^{2+} ions fluctuated in the presence and absence of HA for the entire 32 hours of irradiation. The maximum concentration of Zn^{2+} ions produced in the absence and presence of HA is 14.36 mg/L and 8.57 mg/L at the 6th and 1st hour of irradiation. The dissolution of ZnO nanoparticles in this study is in line with a study by [60], where maximum dissolution was recorded at lower pH (4.8-6.5). Also, visible and UV-light facilitated the dissolution of ZnO nanoparticles in their study. In contrast, our study

reported higher dissolution in the case of larger particle size (< 100 nm) in the absence of HA. Han et al. also proposed the photocatalytic reaction that influenced the dissolution process as follow:

$$ZnO_{(s)} + h\nu \rightarrow ZnO_{(s)} + h^+ + e^- \quad \text{(photocatalysis)} \quad (6)$$

$$h^+ + e^- \rightarrow h\nu \text{ (or heat)} \quad \text{(re-combination)} \quad (7)$$

$$ZnO_{(s)} + 2h^+ \rightarrow Zn^{2+}{}_{(aq)} + \frac{1}{2}O_2 \quad \text{(ZnO photo-dissolution)} \quad (8)$$

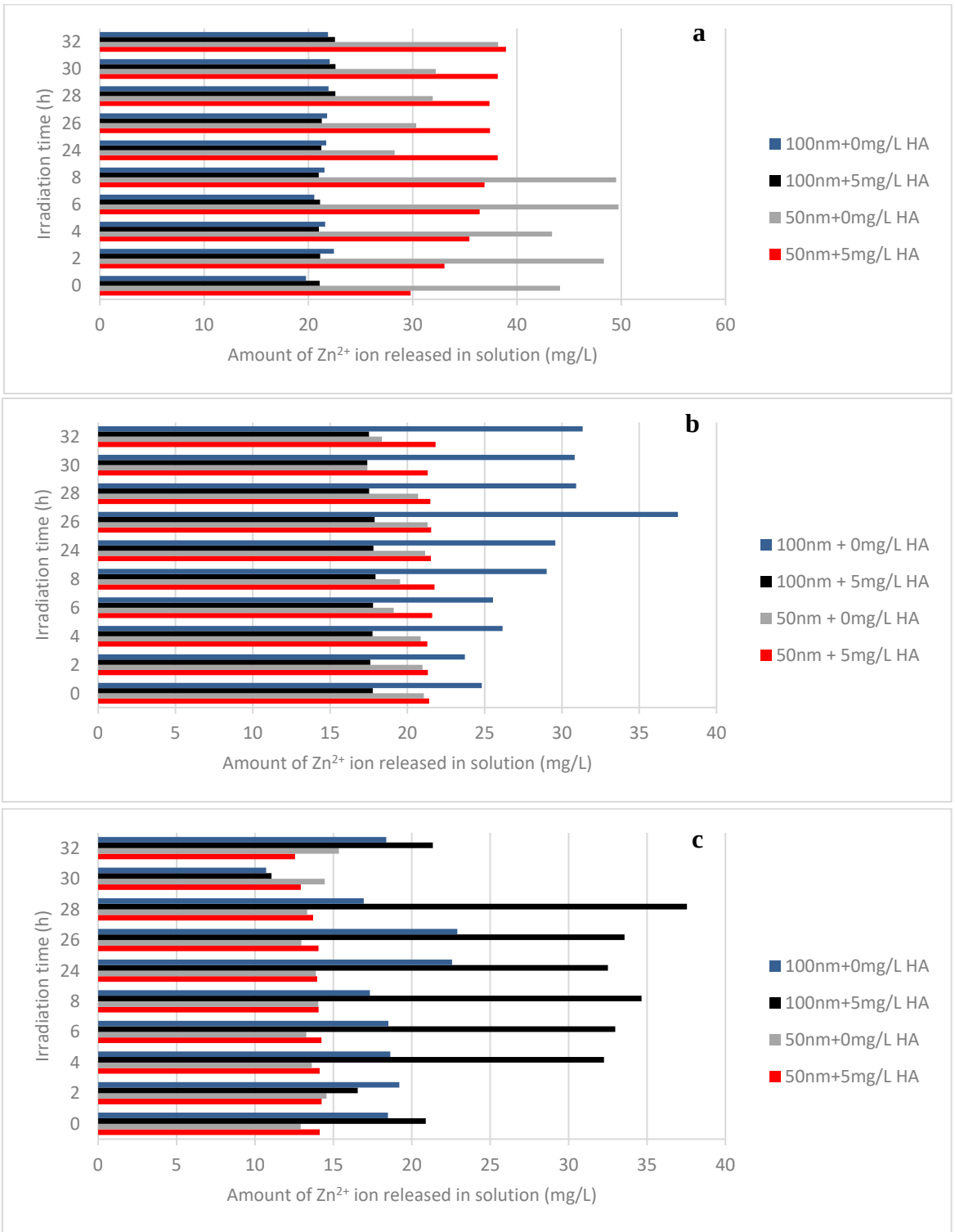

Figure 7. Effect of HA and irradiation time on dissolution of ZnO nanoparticles at (**a**) pH 6; (**b**) pH 7; (**c**) pH 9 for and period of 32 hours [I = 3 mM NaCl].

To study the effect of HA in the dissolution of ZnO nanoparticles, pH 6, pH 7, and pH 9 was chosen since it was a representation of the natural environmental conditions of fresh

surface water (6.5-8.5) and underground water (6-8.5) from the National Water Quality Standards for Malaysia (EQR2006 source).

Figure 7 illustrates the effect of HA, irradiation time on the dissolution of the two ZnO nanoparticle samples at different pH values (6, 7, and 9).

The stability of dissolution of each ZnO nanoparticles at the different pH varies from the different conditions available for each particle. At pH 6, the larger particle size (< 100 nm) in the presence and absence of HA were stable in the ion production as compared to the smaller particles (< 50 nm), which increased in Zn^{2+} ion production with an increase in irradiation time. The maximum concentration of Zn^{2+} ion produced was 38.95 mg/L and 49.94 mg/L for ZnO nanoparticles in the presence and absence of HA. At pH 7, apart from < 100 nm in the absence of HA, the rest of the test samples were stable in their ion production in an aqueous solution. The stabilized Zn^{2+} ion concentration was in the range of 17.77-21.83 mg/L. The maximum concentration of Zn^{2+} ion released by the < 100 nm ZnO nanoparticles in the absence of HA was 37.50 mg/L at the 26th irradiation time. Larger ZnO nanoparticles (< 100 nm) recorded their maximum Zn^{2+} ions concentration (37.55 mg/L) in pH 9. The other samples recorded a stable Zn^{2+} ion concentration both in the presence and absence of HA. This result is in line with a study by [56]. They reported that the solubility of larger-sized ZnO nanoparticles (*n*-ZnO-1) to produce Zn^{2+} ions increased with an increase in HA in a solution of pH 9. The difference might be due to sunlight's presence where the HA may have been photo-degraded due to the electron-hole-pair generated from ZnO nanoparticles when irradiated with sunlight [62]. Literature reported three mechanisms that occur when HA adsorb onto metal oxide nanomaterial surfaces. First, the uniquely high specific surface area of nanoparticles provides HA with a large adsorption space. Secondly, accessibility of the HA molecules to the sites with low hydrophilicity and low negative charge on the particle surface. Finally, the HA adsorption occurs due to the electrostatic attraction and ligand exchange reactions between HA and oxide materials [56].

In comparing the TEM images in Figure 2b and 2d, smaller particles aggregate more in the presence of HA than their larger particles. Although the aggregates tend to present a larger surface area, their interaction with HA hinders their dissolution due to the strong complexation. Previous studies on cerium dioxide interaction with HA concluded that, whenever organic molecules adhere to cerium dioxides, they provide a barrier to aggregation and more dispersion [63].

4. Conclusions

The effects of sunlight and HA on the behavior of ZnO nanoparticles were studied. In the presence of HA, the dissolution of ZnO nanoparticles was higher than the absence of HA. This is because the negative charge of HA changes ZnO nanoparticles' surface charge, preventing the particles from aggregating and precipitating. When exposed to sunlight without HA, the dissolution is stable over the irradiation time. In a combination of both sunlight and HA, the Zn^{2+} ions released doubled as much as without HA. The sorption process of HA onto ZnO nanoparticles was favorable and fitted well by the Langmuir isotherm model.

On the other hand, according to Freundlich's model, the process was unfavorable except for the dataset for pH 11, which had its constant "n" above 1. In conclusion, both factors influenced the ZnO nanoparticles' fate and enhanced the release of Zn^{2+} over time in an aqueous environment. This study also indicates that the fate of ZnO nanoparticles is highly dependent on water chemistry. At higher pH, the dissolution of ZnO was limited by solubility

equilibrium [60]. The pH value a dominant factor, together with sunlight facilitating the ZnO dissolution most probably by degrading the HA.

Funding

This research was supported by the Ministry of Higher Education FRGS/ST01(01)/1208/2014(09) and Universiti Malaysia Sarawak, Tun Openg Chair, F07/TOC/1738/2018.

Acknowledgments

The authors would like to thank colleagues from the Faculty of Resource Science and Technology (FRST), Geochemistry laboratory, Universiti Malaysia Sarawak.

Conflicts of Interest

The authors declare that they have no competing interests regarding the publication of this manuscript. Also, issues of plagiarism, data fabrication and or falsification, double publication, and or submission have been completely observed by the authors. VA Velintine and BS Wee designed the research. VA Velintine carried out the laboratory work. BS Wee, EK Droepenu, SF Chin, and KY Kok conducted the review and editing. Finally, all authors have read and approved the manuscript for publication.

References

1. Ali, I.; Peng, C.; Khan, Z.M.; Naz, I.; Sultan, M.; Ali, M.; Abbasi, I.A.; Islam, T.; Ye, T. Overview of microbes based fabricated biogenic nanoparticles for water and wastewater treatment. *Journal Environmental Management* **2019**, *230*, 128-150, https://doi.org/10.1016/j.jenvman.2018.09.073.
2. Zhu, L.; Li, H.; Xia, P.; Liu, Z.; Xiong, D. Hierarchical ZnO Decorated with CeO2 Nanoparticles as the Direct Z-Scheme Heterojunction for Enhanced Photocatalytic Activity. *ACS Applied Materials & Interfaces* **2018**, *10*, 39679-39687, https://doi.org/10.1021/acsami.8b13782.
3. Hoang Thi, T.T.; Cao, V.D.; Nguyen, T.N.Q.; Hoang, D.T.; Ngo, V.C.; Nguyen, D.H. Functionalized mesoporous silica nanoparticles and biomedical applications. *Materials Science and Engineering: C* **2019**, *99*, 631-656, https://doi.org/10.1016/j.msec.2019.01.129.
4. Pang, W.Y.; Ahmad, A.L.; Zaulkiflee, N.D. Antifouling and antibacterial evaluation of ZnO/MWCNT dual nanofiller polyethersulfone mixed matrix membrane. *Journal Environmental Management* **2019**, *249*, 109358, https://doi.org/10.1016/j.jenvman.2019.109358.
5. Besha, A.T.; Liu, Y.; Bekele, D.N.; Dong, Z.; Naidu, R.; Gebremariam, G.N. Sustainability and environmental ethics for the application of engineered nanoparticles. *Environmental Science & Policy* **2020**, *103*, 85-98, https://doi.org/10.1016/j.envsci.2019.10.013.
6. Yu, J.; Jiang, C.; Guan, Q.; Ning, P.; Gu, J.; Chen, Q.; Zhang, J.; Miao, R. Enhanced removal of Cr(VI) from aqueous solution by supported ZnO nanoparticles on biochar derived from waste water hyacinth. *Chemosphere* **2018**, *195*, 632-640, https://doi.org/10.1016/j.chemosphere.2017.12.12.
7. Danielsson, K.; Gallego-Urrea, J.A.; Hassellov, M.; Gustafsson, S.; Jonsson, C.M. Influence of organic molecules on the aggregation of TiO2 nanoparticles in acidic conditions. *Journal of Nanoparticle Research* **2017**, *19*, 133, http://doi.org/10.1007/s11051-017-3807-9.
8. Arenas-Lago, D.; Monikh, F.A.; Vijver, M.G.; Peijnenburg, W.J. Dissolution and aggregation kinetics of zero valent copper nanoparticles in (simulated) natural surface waters: Simultaneous effects of pH, NOM and ionic strength. *Chemosphere* **2019**, *226*, 841-850, https://doi.org/10.1016/j.chemosphere.2019.03.190.
9. Najim, N.; Rusdi, R.; Hamzah, A.S.; Shaameri, Z.; Mat Zain, M.; Kamarulzaman, N. Effects of the absorption behaviour of ZnO nanoparticles on cytotoxicity measurements. *Journal of Nanomaterials* **2014**, *2014*, http://doi.org/10.1155/2014/694737.
10. Carbery, M.; O'Connor, W.; Palanisami, T. Trophic transfer of microplastics and mixed contaminants in the marine food web and implications for human health. *Environment International* **2018**, *115*, 400-409, https://doi.org/10.1016/j.envint.2018.03.007.
11. Jia, H.-R.; Zhu, Y.-X.; Duan, Q.-Y.; Chen, Z.; Wu, F.-G. Nanomaterials meet zebrafish: Toxicity evaluation and drug delivery applications. *Journal Controlled Release* **2019**, *311-312*, 301-318, https://doi.org/10.1016/j.jconrel.2019.08.022.

12. Dekkers, S.; Ma-Hock, L.; Lynch, I.; Russ, M.; Miller, M.R.; Schins, R.P.F.; Keller, J.; Römer, I.; Küttler, K.; Strauss, V.; De Jong, W.H.; Landsiedel, R.; Cassee, F.R. Differences in the toxicity of cerium dioxide nanomaterials after inhalation can be explained by lung deposition, animal species and nanoforms. *Inhalation Toxicology.* **2018**, *30*, 273-286, https://doi.org/10.1080/08958378.2018.1516834.
13. Oliveira, A.G.; Andrade, J.d.L.; Montanha, M.C.; Lima, S.M.; Andrade, L.H.d.C.; Winkler Hechenleitner, A.A.; Pineda, E.A.G.; Oliveira, D.M.F.d. Decontamination and disinfection of wastewater by photocatalysis under UV/visible light using nano-catalysts based on Ca-doped ZnO. *Journal of Environmental Management* **2019**, *240*, 485-493, https://doi.org/10.1016/j.jenvman.2019.03.124.
14. Liu, Z.; Wang, C.; Hou, J.; Wang, P.; Miao, L.; Lv, B.; Yang, Y.; You, G.; Xu, Y.; Zhang, M.; Ci, H. Aggregation, sedimentation, and dissolution of CuO and ZnO nanoparticles in five waters. *Environmental Science and Pollution Research* **2018**, *25*, 31240-31249, https://doi.org/10.1007/s11356-018-3123-7.
15. Sengul, A.B.; Asmatulu, E. Toxicity of metal and metal oxide nanoparticles: a review. *Environmental Chemistry Letters* **2020**, *18***,** 1659–1683, https://doi.org/10.1007/s10311-020-01033-6.
16. Wahab, R.; Khan, F.; Lutfullah; Singh, R.B.; Kaushik, N.K.; Ahmad, J.; Siddiqui, M.A.; Saquib, Q.; Ali, B.A.; Khan, S.T.; Musarrat, J.; Al-Khedhairy, A.A. Utilization of photocatalytic ZnO nanoparticles for deactivation of safranine dye and their applications for statistical analysis. *Physica E: Low-dimensional Systems and Nanostructures* **2015**, *69*, 101-108, https://doi.org/10.1016/j.physe.2015.01.005.
17. Jiang, J.; Pi, J.; Cai, J. The advancing of zinc oxide nanoparticles for biomedical applications. *Bioinorganic Chemistry & Applications* **2018**, *2018*, https://doi.org/10.1155/2018/1062562.
18. Wahab, R.; Khan, F.; Mishra, Y.K.; Musarrat, J.; Al-Khedhairy, A.A. Antibacterial studies and statistical design set data of quasi zinc oxide nanostructures. *RSC Advances* **2016**, *6*, 32328-32339, https://doi.org/10.1039/C6RA05297E.
19. Sirelkhatim, A.; Mahmud, S.; Seeni, A.; Kaus, N.H.M.; Ann, L.C.; Bakhori, S.K.M.; Hasan, H.; Mohamad, D. Review on Zinc Oxide Nanoparticles: Antibacterial Activity and Toxicity Mechanism. *Nano-Micro Letters* **2015**, *7*, 219-242, https://doi.org/10.1007/s40820-0150040-x.
20. Areerachakul, N.; Sakulkhaemaruethai, S.; Johir, M. A. H.; Kandasamy, J.; Vigneswaran, S. Photocatalytic degradation of organic pollutants from wastewater using aluminium doped titanium dioxide. *Journal of Water Process Engineering* **2019**, *27*, 177-184, https://doi.org/10.1016/j.jwpe.2018.12.006.
21. Birben, N.C.; Paganini, M.C.; Calza, P.; Bekbolet, M. Photocatalytic degradation of humic acid using a novel photocatalyst: Ce-doped ZnO. *Photochemical & Photobiological Sciences* **2017**, *16*, 24-30, https://doi.org/10.1039/C6PP00216A.
22. Bel Hadjltaief, H.; Ben Zina, M.; Galvez, M.E.; Da Costa, P. Photocatalytic degradation of methyl green dye in aqueous solution over natural clay-supported ZnO–TiO2 catalysts. *Journal of Photochemistry & Photobiology A: Chemistry* **2016**, *315*, 25-33, https://doi.org/10.1016/j.jphotochem.2015.09.008.
23. Philippe, A.; Schaumann, G.E. Interactions of Dissolved Organic Matter with Natural and Engineered Inorganic Colloids: A Review. *Environmental Science & Technology* **2014**, *48*, 8946-8962, http://doi.org/10.1021/es502342r.
24. Dziedzic, J.; Wodka, D.; Nowak, P.; Warszyński, P.; Simon, C.; Kumakiri, I. Photocatalytic degradation of the humic species as a method of their removal from water - comparison of UV and artificial sunlight irradiation. *Physicochemical Problems of Mineral Processing* **2010**, *45(1)*, 15-28.
25. Ghaneian, M.T.; Morovati, P.; Ehrampoush, M.H.; Tabatabaee, M. Humic acid degradation by the synthesized flower-like Ag/ZnO nanostructure as an efficient photocatalyst. *Journal of Environmental Health Science and Engineering* **2014**, *12*, 138, http://doi.org/10.1186/s40201-014-0138-y.
26. Tang, W.-W.; Zeng, G.-M.; Gong, J.-L.; Liang, J.; Xu, P.; Zhang, C.; Huang, B.-B. Impact of humic/fulvic acid on the removal of heavy metals from aqueous solutions using nanomaterials: A review. *Science of the Total Environment* **2014**, *468-469*, 1014-1027, http://dx.doi.org/10.1016/j.scitotenv.2013.09.044.
27. Wang, J.; Zhou, Y.; Li, A.; Xu, L. Adsorption of humic acid by bi-functional resin JN-10 and the effect of alkali-earth metal ions on the adsorption. *Journal of Hazardous Materials* **2010**, *176*, 1018-1026, https://doi.org/10.1016/j.jhazmat.2009.11.142.
28. Maiga, D.T.; Nyoni, H.; Nkambule, T.T.; Mamba, B.B.; Msagati, T.A.M. Impact of zinc oxide nanoparticles in aqueous environments: influence of concentrations, natural organic matter and ionic strength. *Inorganic and Nano-Metal Chemistry* **2020**, *50*, 680-692, https://doi.org/10.1080/24701556.2020.1724145.
29. Zhao, Y.; Zhou, W.; Wang, Y.; Gao, B.; Xu, X.; Zhao, Y. The effect of humic acid and bovine serum albumin on the adsorption and stability of ZnO nanoparticles on powdered activated carbon. *Journal of Cleaner Production* **2020**, *251*, 119695, https://doi.org/10.1016/j.jclepro.2019.119695.
30. Huang, J.; Liu, S.; Kuang, L.; Zhao, Y.; Jiang, T.; Liu, S.; Xu, X. Enhanced photocatalytic activity of quantum-dot-sensitized one-dimensionally-ordered ZnO nanorod photocatalyst. *Journal of Environmental Sciences* **2013**, *25*, 2487-2491, http://doi.org/10.1016/S1001-0742(12)60330-1.
31. Shirzad Siboni, M.; Samadi, M.T.; Yang, J.K.; Lee, S.M. Photocatalytic reduction of Cr(VI) and Ni(II) in aqueous solution by synthesized nanoparticle ZnO under ultraviolet light irradiation: a kinetic study. *Environmental Technology* **2011**, *32*, 1573-1579, http://doi.org/10.1080/09593330.201.

32. Zhou, J.; Xu, N.S.; Wang, Z.L. Dissolving Behavior and Stability of ZnO Wires in Biofluids: A Study on Biodegradability and Biocompatibility of ZnO Nanostructures. *Advanced Materials* **2006**, *18*, 2432-2435, https://doi.org/10.1002/adma.200600200.
33. Liu, W.; Li, Y.; Liu, F.; Jiang, W.; Zhang, D.; Liang, J. Visible-light-driven photocatalytic degradation of diclofenac by carbon quantum dots modified porous g-C3N4: Mechanisms, degradation pathway and DFT calculation. *Water Research* **2019**, *151*, 8-19, https://doi.org/10.1016/j.watres.2018.11.084.
34. Ma, H.; Brennan, A.; Diamond, S.A. Photocatalytic reactive oxygen species production and phototoxicity of titanium dioxide nanoparticles are dependent on the solar ultraviolet radiation spectrum. *Environmental Toxicology & Chemistry* **2012**, *31*, 2099-2107, http://doi.org/10.1002/etc.1916.
35. Bian, S.-W.; Mudunkotuwa, I.A.; Rupasinghe, T.; Grassian, V.H. Aggregation and Dissolution of 4 nm ZnO Nanoparticles in Aqueous Environments: Influence of pH, Ionic Strength, Size, and Adsorption of Humic Acid. *Langmuir* **2011**, *27*, 6059-6068, https://doi.org/10.1021/la200570n.
36. Neale, P.A.; Jämting, Å.K.; O'Malley, E.; Herrmann, J.; Escher, B.I. Behaviour of titanium dioxide and zinc oxide nanoparticles in the presence of wastewater-derived organic matter and implications for algal toxicity. *Environmental Science: Nano* **2015**, *2*, 86-93, http://doi.org/10.1039/C4EN00161C.
37. Peng, Y.-H.; Tso, C.-p.; Tsai, Y.-c.; Zhuang, C.-m.; Shih, Y.-h. The effect of electrolytes on the aggregation kinetics of three different ZnO nanoparticles in water. *Science of the Total Environment* **2015**, *530-531*, 183-190, http://doi.org/10.1016/j.scitotenv.2015.05.059,
38. Peng, Y.-H.; Tsai, Y.-C.; Hsiung, C.-E.; Lin, Y.-H.; Shih, Y.-h. Influence of water chemistry on the environmental behaviors of commercial ZnO nanoparticles in various water and wastewater samples. *Journal of Hazardous Materials* **2017**, *322*, 348-356, http://doi.org/10.1016/j.jhazmat.2016.10.003.
39. Degenkolb, L.; Kaupenjohann, M.; Klitzke, S. The Variable Fate of Ag and TiO 2 Nanoparticles in Natural Soil Solutions—Sorption of Organic Matter and Nanoparticle Stability. Water, Air, & Soil Pollution **2019**, *230*, 1-14, https://doi.org/10.1007/s11270-019-4123-z.
40. Velintine, V.; Siong, W.B.; Chin, S.; Kok, K.Y. Transformation of zinc oxide nanoparticles under environmentally relevant conditions: influence of pH and ionic strength. *Transactions on Science and Technology* **2017**, *4(2)*, 123-136, http://tost.unise.org/pdfs/vol4/no2/4x2x123x136.pdf
41. Zhu, M.; Wang, H.; Keller, A.A.; Wang, T.; Li, F. The effect of humic acid on the aggregation of titanium dioxide nanoparticles under different pH and ionic strengths. *Science of the Total Environment* **2014**, *487*, 375-380, https://doi.org/10.1016/j.scitotenv.2014.04.036.
42. Wang, Z.; Cao, M.; Cai, W.; Zeng, H. The effect of humic acid and fulvic acid on adsorption-desorption behavior of copper and zinc in the yellow soil. *AIP Conference Proceedings.* **2017**, *1820*, 040027, https://doi.org/10.1063/1.4977299.
43. Asgari, G.; Ebrahimi, A.; Mohammadi, A.; Ghanizadeh, G. The investigation of humic acid adsorption from aqueous solutions onto modified pumice with hexadecyl trimethyl ammonium bromide. *International Journal of Environmental Health Engineering* **2013**, *2*, 20-20, https://doi.org/10.4103/2277-9183.110176.
44. Javanshah, A.; Saidi, A. Determination of humic acid by spectrophotometric analysis in the soils. *International Journal of Advanced Biotechnology and Research* **2016**, *7*, 19-23.
45. Herbert, N.; Affonso Celso, G.; Marcelo Angelo, C.; Gustavo Ferreira, C.; Daniel, S.; Marcelo Gonçalves dos, S.; Dionir Luiz, B.; Juliano, Z. Adsorption of Cu (II) and Zn (II) from Water by Jatropha curcas L. as Biosorbent. *Open Chemistry* **2016**, *14*, 103-117, https://doi.org/10.1515/chem-2016-0010.
46. Şentürk, İ.; Alzein, M. Adsorption of Acid Violet 17 Onto Acid-Activated Pistachio Shell: Isotherm, Kinetic and Thermodynamic Studies. *Acta Chimica Slovenica* **2020**, *67*, 55-69, http://doi.org/10.17344/acsi.2019.5195.
47. Weber, T.W.; Chakravorti, R.K. Pore and solid diffusion models for fixed-bed adsorbers. *AICHE Journal* **1974**, *20*, 228-238, https://doi.org/10.1002/aic.690200204.
48. Desta, M.B. Batch sorption experiments: Langmuir and Freundlich isotherm studies for the adsorption of textile metal ions onto teff straw (Eragrostis tef) agricultural waste. *Journal of Thermodynamics* **2013**, *2013*, 375830, https://doi.org/10.1155/2013/375830.
49. Domingos, R.F.; Rafiei, Z.; Monteiro, C.E.; Khan, M.A.K.; Wilkinson, K.J. Agglomeration and dissolution of zinc oxide nanoparticles: role of pH, ionic strength and fulvic acid. *Environmental Chemistry* **2013**, *10*, 306-312, http://doi.org/10.1071/EN12202.
50. Dai, H.; Sun, T.; Han, T.; Guo, Z.; Wang, X.; Chen, Y. Aggregation behavior of zinc oxide nanoparticles and their biotoxicity to Daphnia magna: Influence of humic acid and sodium alginate. *Environmental Research* **2020**, *191*, 110086, https://doi.org/10.1016/j.envres.2020.110086.
51. Gasim, M.B.; Khalid, N.A.; Muhamad, H. The influence of tidal activities on water quality of Paka River Terengganu, Malaysia. *Malaysian Journal of Analytical Sciences* **2015**, *19*, 979-990, http://www.ukm.my/mjas/v19_n5/pdf/MuhammadBarzani_19_5_9.pdf
52. Dong, Y.-n.; Li, X.; Huang, Y.; Wang, H.; Li, F. Coagulation and Dissolution of Zinc Oxide Nanoparticles in the Presence of Humic Acid Under Different pH Values. *Environmental Engineering Science* **2016**, *33*, 347-353, http://doi.org/10.1089/ees.2015.0396.

53. Wang, X.; Sun, T.; Zhu, H.; Han, T.; Wang, J.; Dai, H. Roles of pH, cation valence, and ionic strength in the stability and aggregation behavior of zinc oxide nanoparticles. *Journal of Environmental Management.* **2020**, *267*, 110656, https://doi.org/10.1016/j.jenvman.2020.110656.
54. Singh, R.; Dutta, S. The role of pH and nitrate concentration in the wet chemical growth of nano-rods shaped ZnO photocatalyst. *Nano-Structures & Nano-Objects* **2019**, *18*, 100250, https://doi.org/10.1016/j.nanoso.2019.01.009.
55. Han, J.; Qiu, W.; Gao, W. Potential dissolution and photo-dissolution of ZnO thin films. *Journal of Hazardous Materials* **2010**, *178*, 115-122, http://doi.org/10.1016/j.jhazmat.2010.01.050.
56. Han, Y.; Kim, D.; Hwang, G.; Lee, B.; Eom, I.; Kim, P.J.; Tong, M.; Kim, H. Aggregation and dissolution of ZnO nanoparticles synthesized by different methods: Influence of ionic strength and humic acid. *Colloids and Surfaces: Physicochemical Engineering Aspects* **2014**, *451*, 7-15, http://doi.org/10.1016/j.colsurfa.2014.03.030.
57. Oskoei, V.; Dehghani, M.H.; Nazmara, S.; Heibati, B.; Asif, M.; Tyagi, I.; Agarwal, S.; Gupta, V.K. Removal of humic acid from aqueous solution using UV/ZnO nano-photocatalysis and adsorption. *Journal of Molecular Liquids* **2016**, *213*, 374-380, http://dx.doi.org/10.1016/j.molliq.2015.07.052.
58. Khan, R.; Inam, M.A.; Park, D.R.; Zam Zam, S.; Shin, S.; Khan, S.; Akram, M.; Yeom, I.T. Influence of Organic Ligands on the Colloidal Stability and Removal of ZnO Nanoparticles from Synthetic Waters by Coagulation. *Processes* **2018**, *6*, 170, http://dx.doi.org/10.3390/pr6090170.
59. Mekonnen, E.; Yitbarek, M.; Soreta, T.R. Kinetic and thermodynamic studies of the adsorption of Cr(VI) onto some selected local adsorbents. *South African Journal of Chemistry* **2015**, *68*, 45-52, http://doi.org/10.17159/0379-4350/2015/v68a7.
60. Odzak, N.; Kistler, D.; Sigg, L. Influence of daylight on the fate of silver and zinc oxide nanoparticles in natural aquatic environments. *Environmental Pollution* **2017**, *226*, 1-11, http://doi.org/10.1016/j.envpol.2017.04.006.
61. Li, M.; Lin, D.; Zhu, L. Effects of water chemistry on the dissolution of ZnO nanoparticles and their toxicity to Escherichia coli. *Environmental Pollution* **2013**, *173*, 97-102, http://doi.org/10.1016/j.envpol.2012.10.026.
62. Pansamut, G.; Charinpanitkul, T.; Suriyawong, A. Removal of humic acid by photocatalytic process: effect of light intensity. *Engineering Journal* **2013**, *17*, 25-32, http://doi.org/10.4186/ej.2013.17.3.25.
63. Goodhead, R.M.; Johnston, B.D.; Cole, P.A.; Baalousha, M.; Hodgson, D.; Iguchi, T.; Lead, J.R.; Tyler, C.R. Does natural organic matter increase the bioavailability of cerium dioxide nanoparticles to fish? *Environmental Chemistry* **2015**, *12*, 673-682, http://doi.org/10.1071/EN15003.